ARTÍCULO DE INVESTIGACIÓN ORIGINAL

Frequency response of an electric equivalent circuit for a skin type system

F. Gómez-Aguilar,*
J. Bernal-Alvarado,*
J. Rosales-García,**
M. Guía-Calderón,**
T. Córdova-Fraga,*
M. Sosa-Aquino*

* Departamento de Ingeniería Física, DCI, campus León, Universidad de Guanajuato.
** Departamento de Ingeniería Eléctrica, DICIS, campus Irapuato-Salamanca, Universidad de Guanajuato.

Correspondence:
F. Gómez-Aguilar
Loma del Bosque Núm. 103 Col. Lomas del Campestre, 37150. León, Guanajuato.
E-mail: jfga@fisica.ugto.mx

ABSTRACT

In the present work we consider a theoretical representation of an electrical circuit equivalent to a multilayer biological system. The proposed system is of the skin type, containing epidermis, dermis and the subcutaneous tissue. Electrical circuit theory is used, and the behavior of the system is shown in the form of Nyquist and Bode plots. The proposed theoretical approach is a general treatment to describe the bioelectrical transport in a three-layered system, especially in the electrical impedance spectroscopy studies.

Key words: Circuit theory, bioelectric transport, frequency response.

RESUMEN

En el presente trabajo se considera una representación teórica de un circuito eléctrico equivalente a un sistema biológico de múltiples capas. El sistema propuesto es del tipo piel, que contiene la epidermis, la dermis y el tejido subcutáneo. Esto se realiza mediante la teoría de circuitos eléctricos, y el comportamiento del sistema se muestra en forma de diagramas de Nyquist y Bode. El enfoque teórico propuesto es un tratamiento general para describir el transporte bioeléctrico en un sistema de tres capas, especialmente en los estudios de espectroscopia de impedancia eléctrica.

Palabras clave: Teoría de circuitos, transporte bioeléctrico, respuesta en frecuencia.

INTRODUCTION

According to Rigaud[1] who at the beginning of the 20th century began to study the structure of biological tissues based on their electrical properties, biological tissues are conductors and their resistance varies with frequency. The electrical property of any biological tissue depends on its intrinsic structure. In the case of human skin, the impedance can vary with the thickness and moisture content of the organ, the concentration and activity of sweat glands, injuries, age of subject and environmental factors such as temperature and humidity. Electrical impedance studies in biological systems, including human skin, generally, relate to direct measurements of impedance and phase angle as functions of frequency, voltage or current applied[2-6]. In 1974, Burton[7] applied the Bode analysis to measurements of impedance and phase angle of the skin. Through this method, a passive equivalent circuit can be using and considered as a «black box» to plot its impedance and phase angle *versus* frequency. The only necessary assumption is that the system consists only of linear passive elements[7-8]. Although the resulting model is not necessarily unique[7], it describes the system with great precision in the range of frequencies studied. The electrical impedance spectroscopy (EIA) has proven useful in the characterization of biomaterials, recording the behavior of their intrinsic properties by applying a sinusoidal excitation signal. The application of this technique evaluates the bio-

electrical response of the system taking into account the frequency and the output stage[9]. It has also been used to measure biological tissues in which the electrical impedance depends on water content and ionic conduction in the body. It should be noted that the electrical impedance and resistance terms are used without distinction in literature, since the value of the capacitive reactance is very low in humans for the frequencies under study[10]. In terms of frequency, some researches have reported that when the frequency is less than or equal to 10 kHz, the current does not cross the cell membrane, and thus the resistance obtained is relative only to the extracellular mass[11]. This electrical conductivity is greater in adipose tissue compared to fat-free tissue. The resistivity of components such as blood (1.42 Ω/cm) or urine (2 Ω/cm) is low, muscle (20 Ω/cm) and bone (100 Ω/cm) are intermediate, and fat (50 Ω/cm) is high. In the measurement of bioimpedance an electrical stimulus is applied and then the response it produces on a specific region of the body is analyzed. Usually, the stimulus is an alternating current signal of low amplitude intended to measure the electric field or potential difference generated between different parts of the tissue. The relationship between the data of the stimulus applied and the response obtained as a function of frequency provides the impedance spectrum of tissues studied. To extract useful information from the EIA it is necessary to correlate the experimental data with a physiological mechanism, directly, or fit a model with the parameters to establish this relationship with the physiology[12].

On the other hand, the transfer function analysis is a mathematical approach to relate the system response and an input signal (or excitation). The ratio formed by the pattern of the output over the signal by input makes it possible find the zeros and poles, respectively. That is, it represents the boundary region that must not be reached either by the system response or by the excitation signal, at the same time[12]. A state-space representation is a mathematical model of a physical system described by a set of inputs, outputs and state variables related by first order differential equations that are combined in a matrix differential equation of first order. To ignore the number of inputs, outputs and states, the variables are expressed as vectors, and algebraic equations are written in matrix form. The transfer function of a state space model and continuous time-invariant can be obtained as follows: Taking the Laplace transform ℓ of (1)

$$\ell[\dot{x}(t)] = \ell[Ax(t) + Bu(t)] \tag{1}$$

it leads to

$$sX(s) = AX(s) + BU(s) \tag{2}$$

solving for $X(s)$, we have

$$(sI - A)X(s) = BU(s)$$
$$X(s) = (sI - A)^{-1}BU(s) \tag{3}$$

where, I is the identity matrix. This is replaced by $X(s)$ in the output equation

$$Y(s) = CX(s) + DU(s)$$
$$Y(s) = C\left[(SI - A)^{-1} BU(s)\right] + DU(s) \tag{4}$$

The transfer function is defined as the rate of output over input of a system, that is

$$G(s) = \frac{Y(s)}{U(s)} \tag{5}$$

substituting the expression (5) in (4), we have

$$G(s) = C(SI - A)^{-1} B + D \tag{6}$$

To analyze the behavior of the transfer function in the frequency domain, several graphical methods were used such as the Bode plot, which provides a graphical representation of the magnitude and phase *versus* frequency of transfer function[12]. The Nyquist plot is a polar plot of impedance modulus and phase lag. Its usefulness is related to the stability analysis and it is studied with a model described in complex analysis[12]. The Nichols method consists of superimposing the graph of the transfer function in the Nichols chart, thus, it is easy to obtain the maximum amplitude, and the frequency at which it is present, as well as the corresponding point in the phase. One of the biggest drawbacks of working in polar coordinates is that the curve no longer retains its original shape when a modification to the system is made, such as changes in the loop gain. This requires a complete reconstruction of the Nyquist diagram of the system. Then the loop gain is altered, the graphs complete magnitude-phase, run up and down vertically without distortion. When the properties of the phase are changed independently without affecting the gain, the magnitude-phase trace is affected only in the horizontal direction.

In this work we propose an analysis of an electrical circuit equivalent to a three-layered biological model consisting of epidermis, dermis and the subcutaneous tissue. The study is made using the transfer function analysis.

METHODOLOGY

In order to apply the general theory to the skin type system, we propose an equivalent electrical circuit for each component of the skin. The equivalent circuit is the RC circuit with the corresponding values as reported in the literature[13]. Figure 1 shows the schematic diagram to describe the proposed model of the skin, where R_a and R_b are the contact resistances of the electrodes, D_e represents the equivalent circuit of the dermis (R_1, C_1, R_2, C_2, R_3, C_3, G corresponding to the fat equivalent circuit (R_4, C_4, R_5, C_5, R_7, C_7), and finally, the circuit for the muscle (R_6, C_6). Dividing the equivalent circuit in the corresponding layers: dermis, subcutaneous tissue (fat) and muscle, we will consider it as an electrical network with the following parameter values, which in Figure 1 appear as per unit values[12], and correspond to $R_1 = R_b = 0.2$, $R_1 = R_2 = R_3 = 0.4$, $C_1 = C_2 = C_3 = 0.2$, $R_4 = R_5 = R_7 = 0.7$, $C_4 = C_5 = C_7 = 0.3$, $R_6 = 0.5$, $C_6 = 0.5$.

It is known that in biological systems, the module of the impedance is inversely proportional to frequency and does not show phenomena of conversion of electrical energy to magnetic energy[14]. Therefore, it is considered appropriate to model a biological system considering only the capacitive and resistive behavior. Figure 2, shows the circuit equivalent to the first layer of the system; then, applying Kirchhoff's Laws the following representation of state equations is obtained:

$$\dot{x} = Ax + Bu \tag{7}$$

$$y = Cx + Du \tag{8}$$

where

$$A = -\frac{1}{C_1}\left(\frac{1}{R_1} + \frac{1}{R_a + R_b}\right), \quad B = \frac{1}{C_1(R_a + R_b)},$$

$\dot{x}$ is called the state vector, y is the output vector and u is a vector of inputs (or control). A is the matrix of states, B is the input matrix, x is a column vector representing the voltage on the capacitor, C is the matrix output (voltage on the capacitor that models the dermis), $C_1 = 1$ and D are the feedforward matrix, for this model $D = 0$. The values of the parameters of the circuit in Figure 2, correspond to $R_a = R_b = 0.2$, $C_1 = 0.2$ and $R_1 = 0.4$.

Figures 3, 4 and 5 shows the graphs corresponding to the Bode, Nyquist and Nichols plots. The circuit corresponding to the first layer is shown in Figure 1. The transfer function of the first layer is

$$H(s) = \frac{12.5}{s + 25}. \tag{9}$$

Following the above procedure, we obtain the equations of state for the first two layers and for the three layers, with the corresponding Bode, Nyquist and Nichols plots, showing the effect of each layer. In equations (10) and (11) the matrices and vectors for A, B, C and D, for the first two layers and three layers, respectively, are shown.

The matrix representation is a two-dimensional table of numbers consisting of abstract quantities that can be added and multiplied. Equations (10) and (11) describe the system of linear equations and keep track of the coefficients of linear recording data that
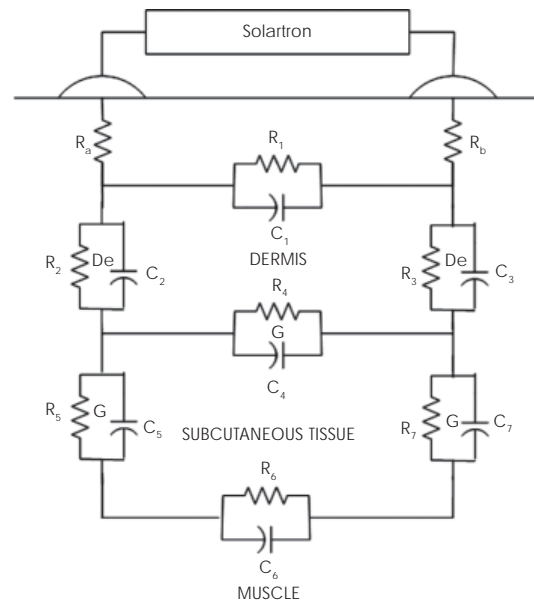

Figure 1. Electrical circuit equivalent to the biological system.
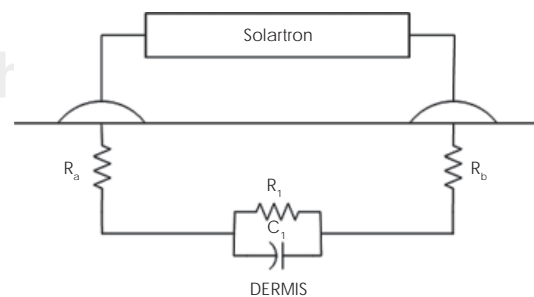

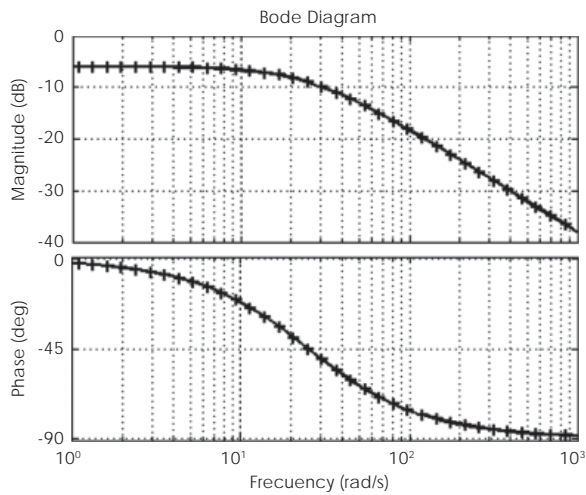**Figure 2.** Electrical circuit equivalent to the first layer of the model.

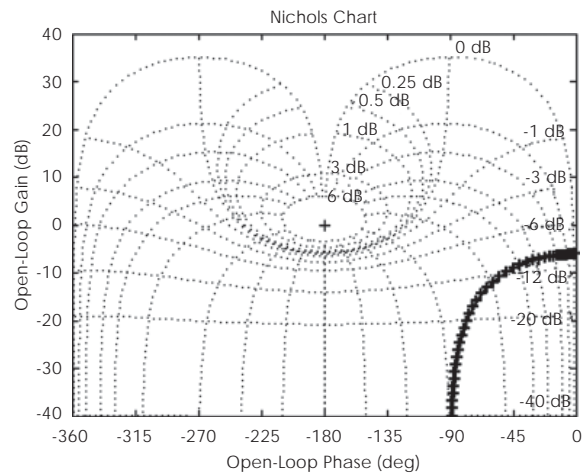Figure 3. Bode diagram for the first layer.

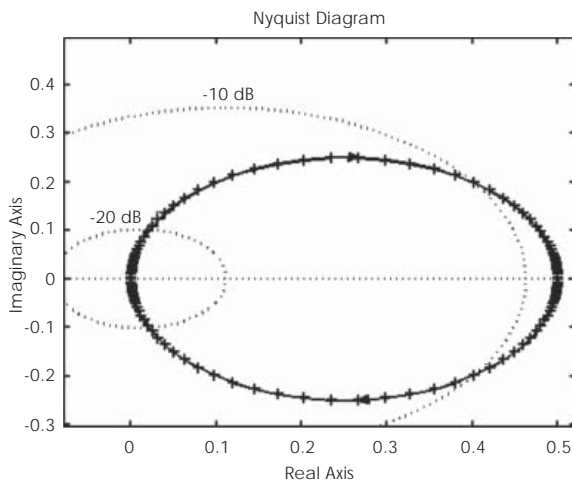Figure 5. Nichols chart for the first layer.

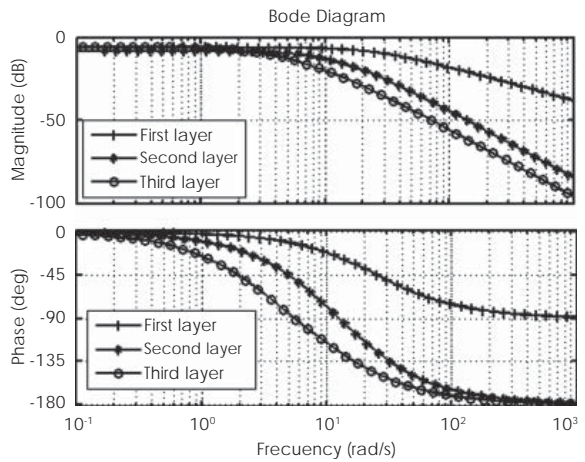Figure 4. Nyquist diagram corresponding to the first layer.

Figure 6. Bode diagram for the first, second and third layers.

$$A = \begin{bmatrix} (R_a + R_b)C_1 & R_a C_2 & R_b C_3 \\ -C_4 & C_2 + C_4 & C_4 \\ -C_4 & C_4 & C_3 + C_4 \end{bmatrix}^{-1} \begin{bmatrix} -1 + \dfrac{R_a + R_b}{R_1} & -\dfrac{R_a}{R_2} & -\dfrac{R_b}{R_3} \\ \dfrac{1}{C_4} & -\left(\dfrac{1}{R_2} + \dfrac{1}{R_4}\right) & \dfrac{1}{R_4} \\ \dfrac{1}{R_4} & -\dfrac{1}{R_4} & -\left(\dfrac{1}{R_3} + \dfrac{1}{R_4}\right) \end{bmatrix}$$

$$B = \left[\left(\frac{1}{R_a + R_b}\right)C_1 \quad 0 \quad 0\right]^T \quad C = [0,0,1] \quad \text{y} \quad D = [0].$$

(10)

$$A = \begin{bmatrix} (R_a+R_b)C_1 & R_aC_2 & R_bC_3 & 0 & 0 \\ -C_4 & C_2+C_4 & C_4 & -C_5 & 0 \\ -C_4 & C_4 & C_2+C_4 & 0 & -C_7 \\ -C_6 & C_6 & C_6 & C_5+C_6 & C_6 \\ C_6 & -C_6 & -C_6 & -C_6 & -(C_6+C_7) \end{bmatrix}^{-1} \begin{bmatrix} -1+\dfrac{R_a+R_b}{R_1} & -\dfrac{R_a}{R_2} & -\dfrac{R_b}{R_3} & 0 & 0 \\ \dfrac{1}{C_4} & -\left(\dfrac{1}{R_2}+\dfrac{1}{R_4}\right) & -\dfrac{1}{R_4} & \dfrac{1}{R_5} & 0 \\ \dfrac{1}{R_4} & -\dfrac{1}{R_4} & -\left(\dfrac{1}{R_3}+\dfrac{1}{R_4}\right) & 0 & \dfrac{1}{R_7} \\ \dfrac{1}{R_6} & -\dfrac{1}{R_6} & -\dfrac{1}{R_6} & -\left(\dfrac{1}{R_5}+\dfrac{1}{R_6}\right) & -\dfrac{1}{R_6} \\ -\dfrac{1}{R_6} & \dfrac{1}{R_6} & \dfrac{1}{R_6} & \dfrac{1}{R_6} & -\left(\dfrac{1}{R_6}+\dfrac{1}{R_7}\right) \end{bmatrix}$$

$$B = \left[\left(\frac{1}{R_a+R_b}\right)C_1 \quad 0 \quad 0 \quad 0 \quad 0\right]^{\mathrm{T}} \quad C = \begin{bmatrix} 0, & 0, & 0, & 0, & 1 \end{bmatrix} \quad \text{and} \quad D = [0]. \tag{11}$$

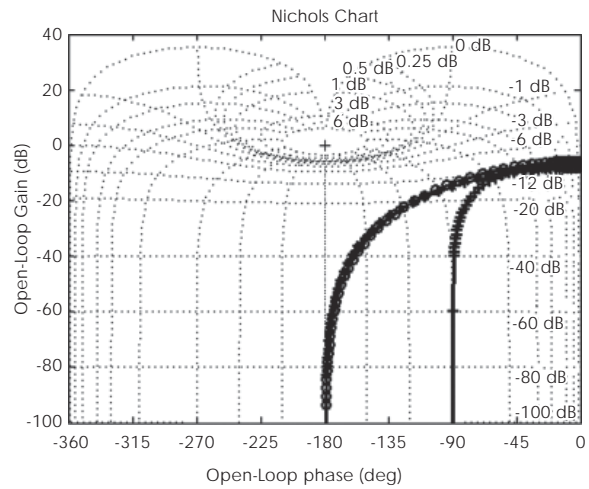**Figure 7.** Nyquist diagram for the first, second and third layers.

Figure 8. Nichols chart for the first, second and third layers.

depend on various parameters. The choice of the values of the circuit parameters is performed taking into account that the array is not indeterminate and that if any row of the matrix is zero, that means that a branch of the circuit has been removed in Figure 1.

Figures 6, 7 and 8 shows the Bode, Nyquist and Nichols diagrams corresponding to the second and third layer, respectively.

In (12), the transfer function of the second layer is shown and in (13) the transfer function to third layer appears.

$$H(s) = \frac{60.88s + 884.5}{s^3 + 41.4s^2 + 546.1s + 2262}. \tag{12}$$

$$H(s) = \frac{16.62s^3 + 631.3s^2 + 7865s + 3198}{s^5 + 53.615s^4 + 1084s^3 + 1018s^2 + 4324s + 6201} \tag{13}$$

In each case, (12) and (13), the input passes through the circuit and reflects a capacitor voltage of study, which is always the farthest from the source. Thus, the transfer function is related to a different output in each case for the same input.

RESULTS AND DISCUSSION

In this work we have analyzed in detail the transfer function of a multilayer system. Figure 3 shows the Bode plot to the magnitude (top graph) and phase

(bottom graph). In the first graph of Figure 3, we see by increasing frequency, from the cutoff frequency (25 rad/s), the magnitude decreases at a rate of 20 dB/decade, while for frequencies below the cutoff magnitude it is almost constant. This means that the current through the dermis is higher with decreasing frequency and is lower when the frequency increases. The attenuation in the first layer is solely due to the resistance of the electrodes. The current flowing through these resistors at low frequencies causes a Joule effect, which raises the temperature and therefore the kinetic energy of the molecules that make up the layer. As the frequency increases, other phenomena occur, such as displacement currents, ionization, polarization, and so on. Concerning phase Figure 3 (bottom graph), we have that by increasing frequency the displacement current and polarization are also increased. This causes a decrease in phase 0° to -90° for very high frequencies. In Figure 4, we see that the spectrum is of the order of -20 dB and varies up to -10 dB. Figure 5, shows that at low frequencies, the attenuation and the phase is about +3 dB and +2.14 dB, respectively.

Significantly, there is not a significant decrease in the rate of change of the magnitude on the frequency, as can be seen from equations (10) and (11), where the number of poles subtracted from the number of zeros is 2. By increasing the number of layers, the output voltage in the layer farthest from the source is attenuated at a faster rat; this is due to the resistance of the previous layers and the increase in frequency, so that the current in the deeper layers of the skin decreases more rapidly with increasing of the frequency. In Figure 6 (bottom graph), the shift in the phase is due to the change in system frequency. Fig 6 shows that adding layers to the model changes the cutoff frequency and the magnitude decreases from 20 dB/decade to 40 dB/decade. For the range of frequency 10 to 100 rad/s a shift in the magnitude and phase is shown, which implies that the proposed circuit has a better definition on these frequencies. In Figure 7, we see that the spectra is of the order of -20 dB and varies up to -10 dB. In Figure 8, a variation of about 2 dB, between the model of one layer and two layers and a phase shift about 3 dB is shown. This difference tends to disappear when increasing the frequency.

The models for electrical impedance spectroscopy are assumed to be linear in their first approximation. The electrical parameters only take a nonlinear behavior in the case of tissue damage due to the excessive power in the supply or in the presence of physical and chemical reactions in the sample induced by the input current (exothermic processes or release of electrons). The electrical conduction, even for alternating current, has impedance that depends on the temperature, which turns the frequency response into a function of temperature[15].

These results suggest that this model can be used for the characterization of biological tissues, since, as shown in Figs. 6, 7 and 8, the Bode plots, Nyquist and Nichols are sensitive to differentiate and characterize the behavior of different bioelectrical layer sets. This include layers that can be described as subcutaneous abnormalities (eg., tumors).

CONCLUSIONS

We have developed the theoretical formalism for the representation of biological systems with successive layers in terms of RC circuits. This model was applied to the description of a real skin system; epidermis, dermis and subcutaneous tissue. Shows the possibility of analysis of frequency response of a multilayer electrical equivalent circuit, taking into account the advantage of the sensitivity of the spectra of Bode, Nyquist and Nichols.

ACKNOWLEDGMENTS

REFERENCES

1. Rigaud B, Hamzaoui L, Chauveau N, Granie M, Scotto Di Rinaldi JP, Morucci JP. "Tissue characterization by impedance: a multifrequency approach". 1994 Physiol Meas 1994; 15: A13-A20.
2. Edelberg R, in "Biophysical Properties of the Skin," H. R. Elden, Editor, pp. 513-550, John Wiley & Sons, New York (1971).
3. Cole KS, Cold Spring Harbor Sump. Quant Biol 1993; 1: 107.
4. Hozawa S. Arch Phys 1928; 219: 111.
5. Plutchik A, Hirsch HR. Science 1963; 141: 927.
6. Stephens WGS. Med Electron Biol Eng 1963; 1: 389.
7. Burton CE, David RM, Portnoy WM, Akers LA. Psychophysiology 1974; 11: 517.
8. Van Valkenburg ME. "Network analysis", 3rd ed., Prentice-Hall, Englewood Cliffs, N.J. (1974).
9. Sosa M, Bernal-Alvarado J, Jiménez-Moreno M, Hernández JC, Gutiérrez-Juárez G, Vargas-Luna M, Huerta M, Villagómez-Castro JC, Palomares P. "Magnetic field influence on electrical properties of human blood measured by impedance spectroscopy". Bioelectromagnetics. Volumen 26, Issue 7, Pages 564–570.
10. Fredix HM, Saris HM, Soeters PB, Wouters FM, Kester DM. "Estimation of body composition by bioelectrical impedance

in cancer patients". European Journal of Clinical Nutrition. Mc Millan Press 2009; 44: 749-752.

11. Hernández F, Salazar CA, Bernal JJ. "Determinación de las propiedades eléctricas en tejido sanguíneo". Ciencia UANL. 2007: 510-515.

12. Dorf, Svoboda, "Circuitos electricos", 6 ed., Alfaomega. Diciembre 2000.

13. Qing-Li Y, Chen P, Haimovitz-Friedman A, Reilly RM, Shun Wong C. "Endothelial Apoptosis Initiates Acute Blood–Brain Barrier Disruption after Ionizing Radiation". Cancer research 2003; 63: 5950–5956.

14. Gabriely S, Lau RW, Gabriel C. "The dielectric properties of biological tissues: III. Parametric models for the dielectric spectrum of tissues". Phys Med Biol 1996; 41: 2271–2293.

15. Bernal-Alvarado J, Alvarez-González R, Palomares P. Electrical characterization of human blood as a function of temperature. AIP Conf Proc 2004; 724: 226-229, USA.